

# Detection of Spin Entanglement via Spin-Charge Separation in Crossed Tomonaga-Luttinger Liquids

Alexander Schroer,<sup>1</sup> Bernd Braunecker,<sup>2</sup> Alfredo Levy Yeyati,<sup>3</sup> and Patrik Recher<sup>1,4</sup>

<sup>1</sup>*Institut für Mathematische Physik, Technische Universität Braunschweig, D-38106 Braunschweig, Germany*

<sup>2</sup>*Scottish Universities Physics Alliance, School of Physics and Astronomy, University of St Andrews, North Haugh, St Andrews KY16 9SS, United Kingdom*

<sup>3</sup>*Departamento de Física Teórica de la Materia Condensada, Condensed Matter Physics Center (IFIMAC), and Instituto Nicolás Cabrera, Universidad Autónoma de Madrid, E-28049 Madrid, Spain*

<sup>4</sup>*Interactive Research Center of Science, Tokyo Institute of Technology, 2-12-1 Ookayama, Meguro, Tokyo 152-8551, Japan*

We investigate tunneling between two spinful Tomonaga-Luttinger liquids (TLLs) realized, e.g., as two crossed nanowires or quantum Hall edge states. When injecting into each TLL one electron of opposite spin, the dc current measured after the crossing differs for singlet, triplet, or product states. This is a striking new non-Fermi liquid feature because the (mean) current in a noninteracting beam splitter is insensitive to spin entanglement. It can be understood in terms of collective excitations subject to spin-charge separation. This behavior may offer an easier alternative to traditional entanglement detection schemes based on current noise, which we show to be suppressed by the interactions.

PACS numbers: 71.10.Pm, 03.65.Ud, 73.40.Gk, 73.63.Nm

Entanglement is a necessary prerequisite for universal quantum computation and certain quantum communication protocols like quantum teleportation or dense coding [1]. The creation of nonlocal pairwise entangled particles has been successfully demonstrated with photons [2–4] by violating a Bell inequality [5, 6]. The same has not yet been demonstrated in transport experiments in a solid state device. In particular, spin-entangled electrons are important candidates, because the electron spin in quantum dots could be used as a qubit [7], with proven promising spin-coherence times [8]. From the theoretical side, Cooper-pair splitters (CPSs) [9–16] were proposed as a potential source of mobile and nonlocal spin-entangled pairs, using the process of crossed Andreev reflection [17, 18]. Experimentally, such CPSs have been built successfully [19–21] with high efficiency [22]. However, the spin entanglement of these correlated pairs has not been demonstrated so far. Several detection schemes for entangled states were proposed based on a violation of a Bell inequality using cross-correlation (noise) measurements [23–29], current measurements in a CPS with spin-filter properties [30], or exploiting beam splitters [31–39] where a bunching or an antibunching behavior in the two-electron scattering process depends on the orbital wave function of the entangled pairs, distinguishing singlets from triplets or product states. The latter is an effect of statistics and holds already for noninteracting electrons. The average current does not carry a signature of entanglement in Fermi-liquid systems [31].

In this Letter we show that the situation is radically different in the case of a beam splitter made of one-dimensional interacting nanowires [40, 41], or, almost equivalently, integer quantum Hall (QH) edge states [42–46]. In these systems, which can conveniently be described as Tomonaga-Luttinger liquids (TLLs) [47, 48],

the average current *is* sensitive to spin entanglement due to the property of spin-charge separation. This is a desirable feature because the current is generally much easier to measure than noise or higher-order correlation functions. An interpretation of the current noise in terms of (anti-)bunching [31] still applies, although Coulomb repulsion reduces the signal. The TLL system allows for an entangler [11, 12, 16] and detector scheme without the need of magnetic elements (spin filters) nor noise-correlation measurements. Experimentally, transport through crossed 1-D conductors has already been demonstrated, including TLL effects [49–52]. We focus on the slightly more general case of nanowires and give details about a QH implementation in the Supplemental Material.

*Model.*—We consider two long nanowires (wire 1 and wire 2), which are connected through a weak tunnel junction at  $x = 0$  (Fig. 1). To the left of the junction, at  $x_1, x_2 < 0$ , electrons are injected pairwise from an entangler, biased with a voltage  $V$ . The temperature is assumed smaller than the bias voltage and can be set to zero for convenience. The rate of injection is sufficiently low that there are no correlations between subsequent electron pairs.

In the TLL left- and right-moving electron modes are expressed as bosonic fluctuations described by the Hamiltonian [53–55]

$$H_0 = \sum_{j\alpha} \int dx \frac{\hbar v_\alpha}{2} \left[ g_\alpha \left( \frac{\partial \phi_{j\alpha}}{\partial x} \right)^2 + \frac{1}{g_\alpha} \left( \frac{\partial \theta_{j\alpha}}{\partial x} \right)^2 \right], \quad (1)$$

with  $\phi$  and  $\theta$  dual phase fields obeying  $[\theta_{j\alpha}(x, t), \phi_{j'\alpha'}(x', t)] = (i/2)\delta_{jj'}\delta_{\alpha\alpha'}\text{sgn}(x - x')$ . In this notation,  $\partial_x \phi_{j\alpha}$  is proportional to the charge current ( $\alpha = \rho$ ) or the spin current ( $\alpha = \sigma$ ) in wire  $j \in \{1, 2\}$  and  $\partial_x \theta_{j\alpha}$  to the corresponding density.

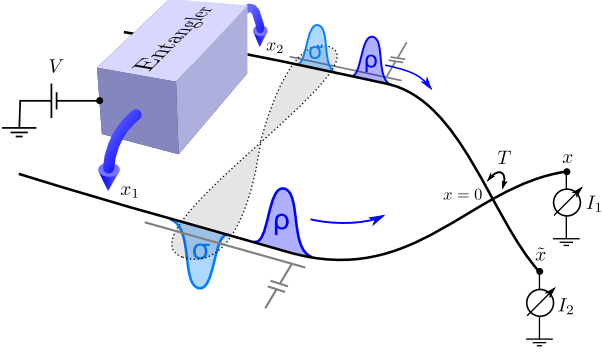


FIG. 1. (Color online) Tunnel junction with amplitude  $T$  at  $x = 0$  between two interacting one-dimensional wires. Via an entangler biased with a voltage  $V$ , two spin-entangled electrons are injected simultaneously at  $x_1$  in wire 1 and at  $x_2$  in wire 2 with an amplitude  $I$ , and subsequently decay into collective spin and charge excitations. The current expectation values  $I_{1,2}$  measured at  $x, \tilde{x}$  at the far opposite side of the junction and their cross correlations are influenced by the entanglement of the original electrons.

Assuming  $SU(2)$  spin invariance, the interaction parameter in the spin sector is  $g_\sigma = 1$ , and in the charge sector,  $g_\rho \equiv g < 1$ . With  $v_F$  the Fermi velocity,  $v_\rho = v_F/g_\rho$  and  $v_\sigma = v_F$  are the velocities of spin and charge excitations. The physical electron field with spin  $s \in \{\uparrow, \downarrow\}$  is  $\psi_{js} = \psi_{jRs} + \psi_{jLs}$  with the right( $R$ )- and left( $L$ )-moving contribution  $\psi_{jR/Ls}(x, t) = (2\pi a)^{-1/2} F_{jR/Ls} \exp[\pm ik_F x + 2\pi i \Phi_{jR/Ls}(x, t)]$  and  $\Phi$  a linear combination of  $\phi$  and  $\theta$  [54, 55]. The Klein factors  $F$  are unitary, anticommuting operators ensuring fermionic commutation relations [54]. The cutoff parameter of the wires,  $a$ , corresponds to their inverse bandwidth.

The tunnel junction at  $x = 0$  is described by the Hamiltonian

$$H_T = T \sum_{\substack{\nu, \nu' \in \{R, L\} \\ s \in \{\uparrow, \downarrow\}}} \left( \psi_{1\nu', s}^\dagger(0) \psi_{2\nu s}(0) + \psi_{2\nu', s}^\dagger(0) \psi_{1\nu s}(0) \right). \quad (2)$$

*Initial state approach.*—First, we include the entangled electron pair as a suitably chosen *initial state* at time  $t_0$  with one electron in each wire at  $x_1$  and  $x_2$ , respectively, on top of the many-particle ground state  $|\rangle$

$$|\varphi\rangle = \frac{\pi a}{\sqrt{2}} \left( \psi_{2\downarrow}^\dagger(x_2) \psi_{1\uparrow}^\dagger(x_1) + e^{i\varphi} \psi_{2\uparrow}^\dagger(x_2) \psi_{1\downarrow}^\dagger(x_1) \right) |\rangle \\ := 2^{-1/2} \sum_{\nu_1, \nu_2} \left( |\nu_1 \uparrow, \nu_2 \downarrow\rangle + e^{i\varphi} |\nu_1 \downarrow, \nu_2 \uparrow\rangle \right). \quad (3)$$

The relative phase  $\varphi$  is the rotation angle between the pure triplet state ( $\varphi = 0$ ) and the pure singlet state ( $\varphi = \pi$ ). We choose  $|x_{1,2}| \gg a$  to avoid initial overlap between the injected electrons and the tunnel contact. Later, we will show that the results of this model carry over to the

case of an applied bias voltage  $V$  by essentially replacing the wave-packet width  $a$  of the state  $|\varphi\rangle$  by  $\hbar v_F/eV$ , where  $e$  is the electron charge.

Every expectation value of an operator  $\mathcal{O}$  with respect to these states can be written as  $\langle \varphi | \mathcal{O} | \varphi \rangle = \mathcal{O}^{\text{dir}} + \cos(\varphi) \mathcal{O}^{\text{exc}}$ , where the *direct* term  $\mathcal{O}^{\text{dir}} = \sum_{\nu_1 \nu_2} \langle \nu_1 \uparrow, \nu_2 \downarrow | \mathcal{O} | \nu_1 \uparrow, \nu_2 \downarrow \rangle$  is the product state contribution, and the *exchange* term  $\mathcal{O}^{\text{exc}} = \sum_{\nu_1 \nu_2} \langle \nu_1 \uparrow, \nu_2 \downarrow | \mathcal{O} | \nu_1 \downarrow, \nu_2 \uparrow \rangle$  is a distinctive indicator of entanglement [31]. Varying  $\varphi$  is a powerful way to identify the exchange contribution in a measurement, which will be discussed later on.

Within this approach, the current expectation value in wire 1 after the injection is given by

$$I_1 = e\Gamma_{2e} \int_{t_0}^{\infty} dt \langle \varphi | I_1(x, t) | \varphi \rangle, \quad (4)$$

with  $x \gg a$ ,  $\Gamma_{2e} \ll v_F a^{-1}$  the rate of injection, and the bosonized current operator [55]  $I_j(x, t) = -\sqrt{2/\pi} \partial_t \theta_j(x, t)$ . Similarly, the zero-frequency cross-correlations between the two wires are

$$S_{12} = \frac{e^2 \Gamma_{2e}}{2} \int_{t_0}^{\infty} dt dt' \langle \varphi | \left\{ \delta I_1(x, t), \delta I_2(\tilde{x}, t') \right\} | \varphi \rangle, \quad (5)$$

where  $\delta I_j = I_j - \langle \varphi | I_j | \varphi \rangle$ .

Treating  $H_T$  as a perturbation [56], the expressions Eqs. (4) and (5) can be evaluated with a standard Keldysh nonequilibrium generating functional approach [57–59]. Besides the zeroth-order contributions (no tunnel processes)  $I_1^{(0)} = -e\frac{\Gamma_{2e}}{2}$  and  $S_{12}^{(0)} = 0$  they yield second order in  $T$  *direct* and *exchange* corrections. The former contain effects due to interactions and spin-charge separation, which are further discussed in the Supplemental Material, but they are not sensitive to entanglement. The latter are

$$I_1^{(2)\text{exc}} = e\Gamma_{2e} \frac{1+g}{2} \\ \times \left[ \langle R \uparrow, R \downarrow | U_{1R \rightarrow 2R}^{(1)\uparrow\uparrow} U_{1R \rightarrow 2R}^{(1)\downarrow} | R \downarrow, R \uparrow \rangle \right. \\ \left. - \langle R \uparrow, R \downarrow | U_{2R \rightarrow 1R}^{(1)\downarrow\downarrow} U_{2R \rightarrow 1R}^{(1)\uparrow} | R \downarrow, R \uparrow \rangle \right], \quad (6)$$

$$S_{12}^{(2)\text{exc}} = -e^2 \Gamma_{2e} \left( \frac{1+g}{2} \right)^2 \\ \times \text{Re} \left[ \langle R \uparrow, R \downarrow | U_{1R \rightarrow 2R}^{(1)\uparrow\uparrow} U_{1R \rightarrow 2R}^{(1)\downarrow} | R \downarrow, R \uparrow \rangle \right. \\ \left. + \langle R \uparrow, R \downarrow | U_{2R \rightarrow 1R}^{(1)\downarrow\downarrow} U_{2R \rightarrow 1R}^{(1)\uparrow} | R \downarrow, R \uparrow \rangle \right]. \quad (7)$$

Here,  $U_{jR \rightarrow kR}^{(1)s} = -i\hbar^{-1} \int_{t_0}^{\infty} dt' H_T(t')|_{jR \rightarrow kR}^s$  is the first-order contribution of the time evolution operator which connects the initial state to a final state in the distant future, including only the parts of the tunnel Hamiltonian  $H_T$  which describe tunneling of right-moving spin  $s$  electrons from wire  $j$  into wire  $k$ . In this way we can

distinguish two events: an electron tunnels out of wire 1 ( $1 \rightarrow 2$ ), and an electron tunnels into wire 1 ( $2 \rightarrow 1$ ). One increases and the other decreases the current, but both add to the noise. Their strength is given by the overlap of the corresponding final state  $U^{(1)s} |\downarrow\uparrow\rangle$  with its spin-flipped counterpart  $\langle\uparrow\downarrow| U^{(1)-s\dagger}$ ; i.e., a process has a large rate if the final state after one tunnel event is mostly invariant under spin flip. This will be a key observation to interpret the results. The factor  $\frac{1+g}{2}$  is caused by charge fractionalization [60]. When measuring the current or noise not in the TLL, but in Fermi liquid reservoirs to the right of the beam splitter, the complete charge will be detected [58, 59, 61–65]. Formally, this corresponds to setting  $g \rightarrow 1$  in the prefactors (but not in the correlation functions) of Eqs. (6) and (7). This, however, only leads to minor quantitative changes, so we will not make the distinction in the following.

In the noninteracting ( $g = 1$ ) and in the symmetric ( $x_1 = x_2$ ) cases, the time integrals in Eqs. (6) and (7) can be solved analytically. At  $g = 1$ , the exchange noise is a Lorentzian of  $d = x_2 - x_1$ ,

$$S_{12}^{(2)\text{exc}} = e^2 \frac{\Gamma_{2e}}{2} \left| \frac{T}{\hbar v_F} \right|^2 \frac{1}{4 + (d/a)^2}, \quad (8)$$

meaning that there can only be an exchange process if the spins meet at the tunnel junction. Like in earlier non-interacting results in energy [31, 34, 35] and time domain [66], nonzero exchange noise requires orbital overlap. Interactions decrease the exchange signal. At  $x_1 = x_2$  the power law  $S_{12}^{(2)\text{exc}} \propto ((1+g)/2)^2 (2g^{-1} + 1)^{-(g^{-1}+g)/2}$  is obtained.

As expected, the exchange current vanishes exactly without interactions, since the two amplitudes in Eq. (6) cancel. This is already true when spin-charge separation is neglected, i.e., when setting  $v_\rho = v_\sigma$ . For  $v_\rho \neq v_\sigma$ , however, a numerical integration of Eq. (6) demonstrates that  $I_1^{(2)\text{exc}}$  is nonzero in general (Fig. 2). This confirms that entanglement can be detected in the many-body system by current measurements only and that the phenomenon of spin-charge separation is essential. It induces a crucial asymmetry between the two competing processes, which goes unnoticed if both are summed up (current noise), but is relevant if they are subtracted (mean current).

The behavior of the exchange current in Fig. 2 can be qualitatively understood in the following way: In the nanowires, the two injected electrons decay each into a collective charge density excitation  $\langle R \uparrow | \partial_x \theta_{i\rho}(x, t) | R \uparrow \rangle = \frac{1+g}{2} \delta_a(x - x_i - v_\rho(t - t_0)) + \frac{1-g}{2} \delta_a(x - x_i + v_\rho(t - t_0))$  and a collective spin density excitation  $\langle R \uparrow | \partial_x \theta_{i\sigma}(x, t) | R \uparrow \rangle = \delta_a(x - x_i - v_\sigma(t - t_0))$ , where  $\delta_a(x) = \frac{1}{\pi} \frac{a}{a^2 + x^2}$  [11, 58]. They propagate with different velocities  $v_{\rho,\sigma}$  and have a nonzero spatial extent  $a$  due to the finite bandwidth. When one of them reaches the tunnel point at  $x = 0$ , there is a charge or spin imbalance across the junction, which is compensated by a

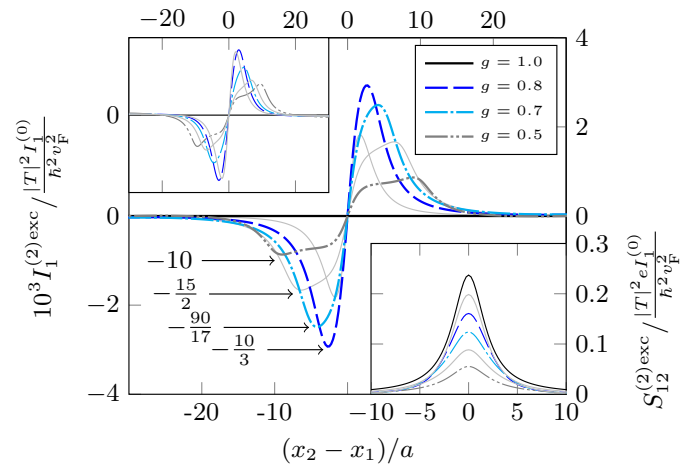


FIG. 2. (Color online) Exchange contributions to the tunnel current in wire 1 and the zero-frequency current cross-correlations between wire 1 and wire 2 (right inset) for different interaction parameters  $g$  and injection distances.  $(x_1 + x_2)/2 = -15a$  is fixed. The exchange contribution to the tunnel current is nonzero if  $x_1 \approx x_2$  because spin-charge separation induces an asymmetry between the two directions of tunneling. The arrow tips indicate the expected positions of the maxima, cf. Eq. (9). Gray lines represent equidistant intermediate  $g$  values. The exchange part of the current noise is finite only if the spins meet at the junction. Left inset: analytic approximation, Eq. (11).

tunneling event: when the spin-down excitation in wire 1 arrives at the junction, either a spin-down electron can tunnel out of wire 1, or a spin-up electron can tunnel into wire 1. So, quite intuitively, spin excitations alone do not create a charge current on average [67]. When, however, the charge excitation in wire 1 arrives at the tunnel contact, the charge imbalance induces only tunneling from wire 1 into wire 2 [first term in Eq. (6)]. It suffices to consider the case in which a spin-down electron tunnels [68]. As illustrated in Fig. 3(a), an additional charge and an additional spin-down excitation are created in wire 2, and a spin-down hole is left behind in wire 1. This final state is invariant under spin flip if the two opposite spin excitations now present in each wire compensate. In wire 1, the spin hole must be compensated by the spin-down excitation from the injection. Because it is created at the position of the charge excitation, spin-charge separation makes this compensation impossible, unless the injection point in wire 1 is near the tunnel junction, so that both excitations are still close. In wire 2, the spin-down excitation produced by tunneling needs to coincide with the spin-up excitation created at injection, so the process is strong if  $x_1/v_\rho = x_2/v_\sigma$ . Following the same reasoning, the competing process  $2 \rightarrow 1$  is strongest if  $x_2/v_\rho = x_1/v_\sigma$ . Unless  $v_\rho = v_\sigma$  these conditions cannot be fulfilled simultaneously, so the two processes do not cancel and the exchange current becomes nonzero [Fig. 3(b)]. Using  $gv_\rho = v_\sigma$ , the two conditions can be

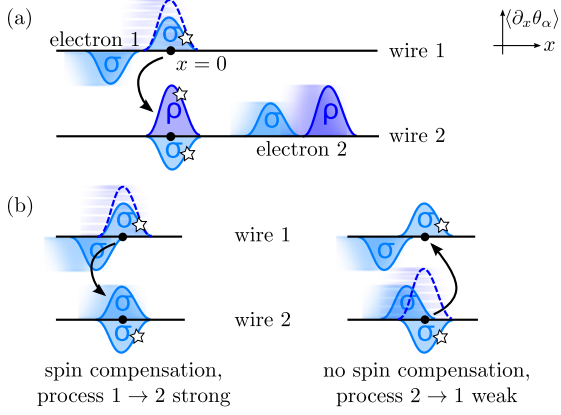


FIG. 3. (Color online) Exchange process. (a)  $x_1 \ll x_2$ . When the charge excitation of electron 1 (dashed line) reaches the tunnel junction at  $x = 0$ , the charge imbalance can trigger a tunnel event. This creates a new charge and a new spin excitation in wire 2 and leaves behind a spin hole in wire 1 (all marked by stars). Spin and charge excitations are drawn with different height for better visibility. (b) For suitable injection points  $x_1/v_\rho = x_2/v_\sigma$  the new spin excitations compensate the one already present in each wire, leading to a strong exchange process. The competing process cannot have spin compensation at the same time and is weak. This asymmetry caused by spin-charge separation gives rise to a finite exchange current.

combined as

$$\frac{x_2 - x_1}{x_2 + x_1} = \pm \frac{g - 1}{g + 1} \quad (9)$$

and become manifest as extrema in the exchange current (indicated by arrows in Fig. 2). Similar peaks reflecting spin-charge separation are already present in the direct terms (cf. Supplemental Material).

Quantitatively, the final state  $1 \rightarrow 2$  is

$$|1 \rightarrow 2\rangle := \sum_t \psi_{2\downarrow}^\dagger(0, t) \psi_{1\downarrow}(0, t) \psi_{1\downarrow}^\dagger(x_1, t_0) \psi_{2\uparrow}^\dagger(x_2, t_0) | \rangle, \quad (10)$$

where  $t \in \{x_1/v_\rho, x_1/v_\sigma, x_2/v_\sigma\}$  is summed over all possible tunnel times (including the spin-induced events to allow for interference effects). The corresponding process strength is  $P_{1 \rightarrow 2} := \langle 1 \widetilde{\rightarrow} 2 | 1 \rightarrow 2 \rangle$ , where  $|1 \widetilde{\rightarrow} 2\rangle$  is the spin-flipped final state, obtained by flipping all spin indices in Eq. (10). Constructing  $P_{2 \rightarrow 1}$  analogously, the exchange current becomes

$$I_1^{(2)\text{exc}} \approx e\Gamma_{2e} \left| \frac{T}{\hbar v_F} \right|^2 \frac{1+g}{2} (P_{2 \rightarrow 1} - P_{1 \rightarrow 2}). \quad (11)$$

All features of the numerics are reproduced by this expression (Fig. 2, left inset). From the explicit form of  $P_{i \rightarrow j}$ , which is calculated in the Supplemental Material, we extract that the exchange current decays as  $I^{(2)\text{exc}} \propto |x_1 + x_2|^{-3}$ .

*Biased injection.*—Time controlled pointlike pair injection into QH edge states has recently been demonstrated with charge pumps [69]. A CPS operated at a constant voltage, on the other hand, can be modeled by a pair-tunneling Hamiltonian which takes into account a voltage induced phase difference [70] instead of the initial state approach. The voltage gives rise to a length scale  $\sim \hbar v_F / eV$ . At large bias,  $eV \rightarrow \hbar v_F a^{-1}$ , the injection becomes as pointlike as allowed by the bandwidth and we recover the results of the initial state approach. At low voltages, it follows from standard renormalization group arguments that physical quantities like the current depend on the ratio of  $x_{1,2}$  and the length scale set by the voltage (Supplemental Material). In particular, the exchange currents at two voltages  $V, V'$  are related through

$$I_{1 x_1, x_2}^{\text{exc}}(V) \approx \left( \frac{V}{V'} \right)^{g^{-1} + g - 1} I_{1 \frac{V}{V'} x_1, \frac{V}{V'} x_2}^{\text{exc}}(V'). \quad (12)$$

This means that in order to access the  $x_{1,2}$  dependency illustrated in Fig. 2 experimentally, it is not necessary to actually move the injection points. Rather, varying voltages can be applied to a fixed geometry sample (cf. Supplemental Material). In a QH realization, the length of different edges can be fine-tuned by appropriate gating, which additionally gives direct access to  $x_{1,2}$ .

To estimate the signal strength, we assume that the distance between the tunnel junction and the injection points is on the order of the length set by the bias voltage,  $x_1 = \hbar v_F / eV$  and  $x_2 = 3\hbar v_F / eV$ . At smaller distances injection and tunneling cannot be regarded as distinct events. While not changing the physics, this considerably complicates quantitative predictions. At much larger distances, disorder and spin decoherence may become relevant. Employing the scaling relation [Eq. (12)], we obtain  $I_{1 x_1, x_2}^{\text{exc}}(V) \approx e^2 \hbar^{-1} V I_{1 x_1=a, x_2=3a}^{\text{exc, init}}(eV/a)$ , where  $I_1^{\text{exc, init}}$  is the exchange current obtained in the initial state approach. To remove the explicit dependency on the cutoff we have used  $g^{-1} + g - 1 \approx 1$ , a valid approximation for a common nanowire interaction parameter  $g = 0.8$ . A CPS is operated at voltages below the superconducting energy gap of about 1 meV (Nb), such as  $V \sim 0.1$  mV. For a total transmission  $|I|^2 |T|^2 \sim 10^{-2} \hbar^4 v_F^4$ , with  $I$  the injection amplitude, the exchange current is on the order of a few pA, a well-accessible value in experiments. With  $v_F = 10^5$  m/s, the injection distances become  $|x_1| \sim 500$  nm and  $|x_2| \sim 1500$  nm.

The primary challenge when designing an entanglement detection scheme which is not based on the violation of a Bell-type inequality is to isolate the exchange contribution from the background given by the direct contributions and measurement noise. This is particularly true for the exchange current, which is 2 to 3 orders of magnitude smaller than the background. When changing the phase angle  $\varphi$  linearly, the exchange contribution oscillates and can be isolated easily via lock-in

amplification from the direct signal, which remains unaffected, cf. Eq. (3). All other parameters can then remain fixed. One way to influence  $\varphi$  is given by the Rashba spin-orbit interaction [71] present in nanowires: when applying a transversal electric field  $E$  (illustrated by the gray back gates in Fig. 1), spin-up and spin-down electrons acquire different Fermi vectors  $k_F \pm k_R$  [32] where  $k_R = 2\pi/\lambda_R \propto E$  is tunable via back gates [72, 73]. In this way, until reaching the tunnel junction a relative phase  $\varphi = 4\pi(x_1 - x_2)/\lambda_R \propto E$  is collected. Recent experiments on InAs wires show that the Rashba length  $\lambda_R$  can become as short as 150 nm [74] which allows for several oscillation periods at the beam splitter size as estimated above. When ramping the electric field  $E$  up and down in a triangular fashion, the exchange current oscillates continuously. Entanglement can thus be detected without any magnetic element or correlation measurement.

To conclude, we have demonstrated how, due to spin-charge separation, the hallmark of TLLs, spin entanglement affects the average charge current in an electronic beam splitter. The underlying mechanism can be fully understood in terms of collective excitations. In addition to traditional entanglement detection schemes based on spin filters and correlation measurements, which have proven to be notoriously difficult to implement, this effect allows for a promising new approach.

We thank A. Baumgartner, F. Dolcini, T. Fujisawa, and B. Trauzettel for helpful discussions and comments. We acknowledge the support by the EU-FP7 project SE2ND, No. 271554, the DFG Grant No. RE 2978/1-1 (PR), and Spanish MINECO through grant FIS2011-26156 (ALY).

## SUPPLEMENTAL MATERIAL

We give further details about the construction of the generating functional and the nonequilibrium perturbative expansion within the initial state approximation. The direct tunnel contributions to the current and to the current noise are discussed with a special focus on features induced by spin-charge separation. We give the full analytic approximation of the exchange current discussed in the main text and confirm the validity of the initial state approximation and the bias-dependent scaling behavior numerically. The  $I(V)$  and  $G(V)$  behaviors implied by the scaling behavior are plotted. An alternative implementation using a quantum Hall sample of Corbino geometry is discussed. For brevity we set  $a = e = \hbar = v_F = 1$  in intermediate results.

## GENERATING FUNCTIONAL AND PERTURBATION THEORY

It is convenient to introduce a contour-ordered generating functional

$$\begin{aligned} Z_{x_1, x_2}^\varphi &= \langle \varphi | \mathcal{T}_C e^{\int dx \int_C dt \sum_{i\nu s} j_{i\nu s}(x, t) \Phi_{i\nu s}(x, t)} | \varphi \rangle \\ &= Z_{x_1, x_2}^{\text{dir}} + \cos(\varphi) Z_{x_1, x_2}^{\text{exc}}, \end{aligned} \quad (\text{S1})$$

where  $i \in \{1, 2\}$  labels the wire,  $\nu \in \{R, L\} \equiv \{1, -1\}$  distinguishes left and right-movers,  $s \in \{\uparrow, \downarrow\} \equiv \{1, -1\}$  is the spin index and  $j$  a source field. Time-ordering  $\mathcal{T}_C$  and the integral in the exponential are performed along the Keldysh contour from  $t_0$  to  $\infty$  (+ branch) and back again (− branch). The relation between the different phase fields reads

$$\Phi_{i\nu s} = \left( \phi_{i\rho} + s\phi_{i\sigma} + \nu(\theta_{i\rho} + s\theta_{i\sigma}) \right). \quad (\text{S2})$$

We can rewrite the current as

$$I_1 = -\Gamma_{2e} \int dt \sum_{\nu s} \nu \partial_t \frac{\delta Z_{x_1, x_2}^\varphi}{\delta j_{1\nu s}(x, t^+)} \Big|_{j=0}, \quad (\text{S3})$$

and the current noise as

$$\begin{aligned} S_{12} &= \Gamma_{2e} \text{Re} \int dt d\tilde{t} \sum_{\nu\tilde{\nu} s\tilde{s}} \nu\tilde{\nu} \partial_t \partial_{\tilde{t}} \\ &\left( \frac{\delta^2 Z_{x_1, x_2}^\varphi}{\delta j_{1\nu s}(x, t^-) \delta j_{2\tilde{\nu}\tilde{s}}(\tilde{x}, \tilde{t}^+)} \right. \\ &\quad \left. - \frac{\delta Z_{x_1, x_2}^\varphi}{\delta j_{1\nu s}(x, t^-)} \frac{\delta Z_{x_1, x_2}^\varphi}{\delta j_{2\tilde{\nu}\tilde{s}}(\tilde{x}, \tilde{t}^+)} \right) \Big|_{j=0}. \end{aligned} \quad (\text{S4})$$

Like any expectation value, the generating functional can be written as a direct and an exchange term. Explicitly, they read in the interaction picture with respect to  $H_0$

$$\begin{aligned} Z_{x_1, x_2}^{\text{dir/exc}} &= \frac{1}{4} \sum_{\nu_1 \nu'_1 \nu_2 \nu'_2} \langle \mathcal{T}_C F_{1\nu_1 \uparrow} F_{2\nu_2 \downarrow} F_{2\nu'_2 \downarrow/\uparrow}^\dagger F_{1\nu'_1 \uparrow/\downarrow}^\dagger \rangle \\ &\exp \left[ \int dx \int_C dt \sum_{i\nu s} j_{i\nu s}(x, t) \Phi_{i\nu s}(x, t) \right. \\ &\quad + 2\pi i (\Phi_{1\nu_1 \uparrow}(x_1, t_0^-) - \Phi_{1\nu'_1 \uparrow/\downarrow}(x_1, t_0^+)) \\ &\quad + 2\pi i (\Phi_{2\nu_2 \downarrow}(x_2, t_0^-) - \Phi_{2\nu'_2 \downarrow/\uparrow}(x_2, t_0^+)) \\ &\quad \left. - i \int_C dt H_T \right]_0 \end{aligned} \quad (\text{S5})$$

with the ground state expectation value  $\langle \cdot \rangle_0$  of the unperturbed system. To express all quantities of interest we will use the contour time-ordered correlation functions,

following ref. [53],

$$\begin{aligned}
C_{ss'}^{\nu\nu'}(x, t; x', t') &= \langle \Gamma_C \Phi_{i\nu s}(x, t) \Phi_{i\nu' s'}(x', t') \rangle \\
&= -\frac{1}{32\pi^2} \left( (g_\rho^{-1} + \nu + \nu' + \nu\nu' g_\rho) \log\left(\frac{2\pi}{L} f_{\rho+}\right) \right. \\
&\quad \left. + (g_\rho^{-1} - \nu - \nu' + \nu\nu' g_\rho) \log\left(\frac{2\pi}{L} f_{\rho-}\right) \right. \\
&\quad \left. + ss'(\rho \rightarrow \sigma) \right), \tag{S6}
\end{aligned}$$

where

$$f_{\alpha\pm} := -i \operatorname{sgn}_C(t-t') (\pm(x-x') - v_\alpha(t-t')) + a. \tag{S7}$$

The contour sign function  $\operatorname{sgn}_C(t-t')$  is 1 whenever  $t$  is later on the Keldysh contour than  $t'$ , and  $-1$  otherwise.

When expanding  $Z$  in the tunnel amplitude, the additional Klein factors from the tunnel Hamiltonian impose strong constraints on the internal quantum numbers of the tunnel events. Using the Debye-Waller identity  $\langle e^{\sum x_i} \rangle = e^{\frac{1}{2} \langle (\sum x_i)^2 \rangle}$  we arrive at

$$\begin{aligned}
Z_{x_1, x_2}^{(0)\text{dir}} &= \frac{1}{4} \sum_{\nu_1 \nu_2} \exp \left[ \frac{1}{2} \int dx dx' \int_C dt dt' \sum_{i\nu\nu' s s'} j_{i\nu s}(x, t) j_{i\nu' s'}(x', t') C_{ss'}^{\nu\nu'}(x, t; x', t') \right. \\
&\quad \left. + 2\pi i \int dx \int_C dt \sum_{\nu s} \left[ j_{1\nu s}(x, t) \left( C_{s\uparrow}^{\nu\nu_1}(x, t; x_1, t_0^-) - C_{s\uparrow}^{\nu\nu_1}(x, t; x_1, t_0^+) \right) \right. \right. \\
&\quad \left. \left. + j_{2\nu s}(x, t) \left( C_{s\downarrow}^{\nu\nu_2}(x, t; x_2, t_0^-) - C_{s\downarrow}^{\nu\nu_2}(x, t; x_2, t_0^+) \right) \right] \right], \tag{S8}
\end{aligned}$$

$$\begin{aligned}
Z_{x_1, x_2}^{(2)\text{dir}} &= -|T|^2 \int_C dt' dt'' \sum_{\nu_1 \nu_2} \exp \left[ \frac{1}{2} \int dx dx' \int_C dt dt' \sum_{i\nu\nu' s s'} j_{i\nu s}(x, t) j_{i\nu' s'}(x', t') C_{ss'}^{\nu\nu'}(x, t; x', t') \right] \\
&\quad \times \left[ \sum_{\nu' \nu'' s'} \exp \left[ + 2\pi i \int dx \int_C dt \sum_{\nu s} \left[ j_{1\nu s}(x, t) \left( C_{s\uparrow}^{\nu\nu_1}(x, t; x_1, t_0^-) - C_{s\uparrow}^{\nu\nu_1}(x, t; x_1, t_0^+) \right) \right. \right. \right. \\
&\quad \left. \left. + C_{ss'}^{\nu\nu'}(x, t; 0, t') - C_{ss'}^{\nu\nu'}(x, t; 0, t'') \right) \right. \\
&\quad \left. \left. + j_{2\nu s}(x, t) \left( C_{s\downarrow}^{\nu\nu_2}(x, t; x_2, t_0^-) - C_{s\downarrow}^{\nu\nu_2}(x, t; x_2, t_0^+) \right) \right. \right. \\
&\quad \left. \left. - C_{ss'}^{\nu\nu''}(x, t; 0, t') + C_{ss'}^{\nu\nu''}(x, t; 0, t'') \right] \right] \\
&\quad \times \langle \nu_1 \uparrow, \nu_2 \downarrow | \Gamma_C \mathcal{H}_{1\nu' \rightarrow 2\nu''}^{T s'}(t') \mathcal{H}_{2\nu'' \rightarrow 1\nu'}^{T s'}(t'') | \nu_1 \uparrow, \nu_2 \downarrow \rangle \\
&\quad + \sum_{\nu'} \exp \left[ + 2\pi i \int dx \int_C dt \sum_{\nu s} \left[ j_{1\nu s}(x, t) \left( C_{s\uparrow}^{\nu\nu_1}(x, t; x_1, t_0^-) - C_{s\uparrow}^{\nu, -\nu_1}(x, t; x_1, t_0^+) \right) \right. \right. \\
&\quad \left. \left. + C_{ss'}^{\nu, -\nu_1}(x, t; 0, t') - C_{ss'}^{\nu, -\nu_1}(x, t; 0, t'') \right) \right. \\
&\quad \left. \left. + j_{2\nu s}(x, t) \left( C_{s\downarrow}^{\nu\nu_2}(x, t; x_2, t_0^-) - C_{s\downarrow}^{\nu\nu_2}(x, t; x_2, t_0^+) \right) \right. \right. \\
&\quad \left. \left. - C_{ss'}^{\nu\nu'}(x, t; 0, t') + C_{ss'}^{\nu\nu'}(x, t; 0, t'') \right] \right] \\
&\quad \times \langle \nu_1 \uparrow, \nu_2 \downarrow | \Gamma_C \mathcal{H}_{1, -\nu_1 \rightarrow 2\nu'}^{T s'}(t') \mathcal{H}_{2\nu' \rightarrow 1\nu_1}^{T s'}(t'') | -\nu_1 \uparrow, \nu_2 \downarrow \rangle \\
&\quad + \sum_{\nu'} \exp \left[ + 2\pi i \int dx \int_C dt \sum_{\nu s} \left[ j_{1\nu s}(x, t) \left( C_{s\uparrow}^{\nu\nu_1}(x, t; x_1, t_0^-) - C_{s\uparrow}^{\nu\nu_1}(x, t; x_1, t_0^+) \right) \right. \right. \\
&\quad \left. \left. + C_{ss'}^{\nu\nu'}(x, t; 0, t') - C_{ss'}^{\nu\nu'}(x, t; 0, t'') \right) \right. \\
&\quad \left. \left. + j_{2\nu s}(x, t) \left( C_{s\downarrow}^{\nu\nu_2}(x, t; x_2, t_0^-) - C_{s\downarrow}^{\nu, -\nu_2}(x, t; x_2, t_0^+) \right) \right. \right. \\
&\quad \left. \left. - C_{ss'}^{\nu\nu_2}(x, t; 0, t') + C_{ss'}^{\nu, -\nu_2}(x, t; 0, t'') \right] \right] \\
&\quad \times \langle \nu_1 \uparrow, \nu_2 \downarrow | \Gamma_C \mathcal{H}_{1\nu' \rightarrow 2\nu_2}^{T s'}(t') \mathcal{H}_{2, -\nu_2 \rightarrow 1\nu'}^{T s'}(t'') | \nu_1 \uparrow, -\nu_2 \downarrow \rangle \tag{S9}
\end{aligned}$$

and

$$\begin{aligned}
Z_{x_1, x_2}^{(2)\text{exc}} = & -|T|^2 \int_{\mathcal{C}} dt' dt'' \sum_{\nu_1 \nu_1' \nu_2 \nu_2'} \exp \left[ \frac{1}{2} \int dx dx' \int_{\mathcal{C}} dt dt' \sum_{i \nu \nu' s s'} j_{i \nu s}(x, t) j_{i \nu' s'}(x', t') C_{s s'}^{\nu \nu'}(x, t; x', t') \right. \\
& + 2\pi i \int dx \int_{\mathcal{C}} dt \sum_{\nu s} \left[ j_{1 \nu s}(x, t) \left( C_{s \uparrow}^{\nu \nu_1}(x, t; x_1, t_0^-) - C_{s \downarrow}^{\nu \nu_1}(x, t; x_1, t_0^+) \right) \right. \\
& \quad + C_{s \downarrow}^{\nu \nu_1}(x, t; 0, t') - C_{s \uparrow}^{\nu \nu_1}(x, t; 0, t'') \\
& \quad + j_{2 \nu s}(x, t) \left( C_{s \downarrow}^{\nu \nu_2}(x, t; x_2, t_0^-) - C_{s \uparrow}^{\nu \nu_2}(x, t; x_2, t_0^+) \right) \\
& \quad \left. \left. - C_{s \downarrow}^{\nu \nu_2}(x, t; 0, t') + C_{s \uparrow}^{\nu \nu_2}(x, t; 0, t'') \right) \right] \\
& \times \langle \nu_1 \uparrow, \nu_2 \downarrow | T_{\mathcal{C}} \mathcal{H}_{1 \nu_1' \rightarrow 2 \nu_2}^{T \downarrow}(t') \mathcal{H}_{2 \nu_2' \rightarrow 1 \nu_1}^{T \uparrow}(t'') | \nu_1' \downarrow, \nu_2' \uparrow \rangle, \tag{S10}
\end{aligned}$$

where we have decomposed the tunnel Hamiltonian  $H_T = T \sum_{i \nu \nu' s} \mathcal{H}_{i \nu \rightarrow i \nu'}^{T s}$  into the processes in which a  $\nu$ -moving spin- $s$  electron tunnels from wire  $i$  into wire  $\bar{i}$ , becoming a  $\nu'$ -mover. The relevant amplitudes are

$$\begin{aligned}
\langle \nu_1 \uparrow, \nu_2 \downarrow | T_{\mathcal{C}} \mathcal{H}_{1 \nu_1' \rightarrow 2 \nu_2}^{T s}(t') \mathcal{H}_{2 \nu_2' \rightarrow 1 \nu_1}^{T s}(t'') | \nu_1 \uparrow, \nu_2 \downarrow \rangle = & \frac{a^{(g^{-1}+g-2)/2}}{4(2\pi)^2} \left[ f_{\rho}^{-\frac{g^{-1}+g}{2}} f_{\sigma}^{-1} \right] (0, t'; 0, t'') \\
& \times \Xi_{\nu_1 \nu s}(x_1, t_0^-; 0, t') \Xi_{\nu_1 \nu s}(x_1, t_0^+; 0, t'') \Xi_{\nu_1 \nu s}^{-1}(x_1, t_0^-; 0, t'') \Xi_{\nu_1 \nu s}^{-1}(x_1, t_0^+; 0, t') \\
& \times \Xi_{\nu_2 \nu' -s}(x_2, t_0^-; 0, t') \Xi_{\nu_2 \nu' -s}(x_2, t_0^+; 0, t'') \Xi_{\nu_2 \nu' -s}^{-1}(x_2, t_0^-; 0, t'') \Xi_{\nu_2 \nu' -s}^{-1}(x_2, t_0^+; 0, t'') \tag{S11}
\end{aligned}$$

and

$$\begin{aligned}
\langle R \uparrow, R \downarrow | T_{\mathcal{C}} \mathcal{H}_{1 R \rightarrow 2 R}^{T \downarrow}(t') \mathcal{H}_{2 R \rightarrow 1 R}^{T \uparrow}(t'') | R \downarrow, R \uparrow \rangle = & -\frac{a^{(g^{-1}+g+2)/2}}{4(2\pi)^2} \left[ f_{\rho}^{-\frac{g^{-1}+g}{2}} f_{\sigma} \right] (0, t'; 0, t'') \\
& \times \Xi_{R R \downarrow}(x_1, t_0^-; 0, t') \Xi_{R R \downarrow}(x_1, t_0^+; 0, t'') \Xi_{R R \downarrow}(x_2, t_0^-; 0, t'') \Xi_{R R \downarrow}(x_2, t_0^+; 0, t') \\
& \times \Xi_{R R \uparrow}^{-1}(x_1, t_0^-; 0, t'') \Xi_{R R \uparrow}^{-1}(x_1, t_0^+; 0, t') \Xi_{R R \uparrow}^{-1}(x_2, t_0^-; 0, t') \Xi_{R R \uparrow}^{-1}(x_2, t_0^+; 0, t'') \tag{S12}
\end{aligned}$$

with the abbreviation

$$\Xi_{\nu \nu' s} = f_{\rho+}^{\frac{g^{-1}+\nu+\nu'+\nu\nu'g}{s}} f_{\rho-}^{\frac{g^{-1}-\nu-\nu'+\nu\nu'g}{s}} f_{\sigma\nu}^{\frac{1+\nu\nu'}{4s}}. \tag{S13}$$

Substituting this into Eqs. (S3) and (S4), the functional derivatives and the  $t$  and  $\tilde{t}$ -integral can be performed in a straightforward fashion. For the integration we use that  $x, \tilde{x} \gg a$ . The result is independent of the measurement points  $x$  and  $\tilde{x}$  and the measurement times  $t$  and  $\tilde{t}$ , because, irrespective of when the electrons are injected and of how far they have to travel before being measured, they will be detected eventually. More importantly, in the second order corrections only terms for which the tunneling times  $t'$  and  $t''$  lie on different branches of the Keldysh contour survive. Identifying the integral over the first order tunnel Hamiltonian with the interaction picture time evolution operator,  $-iT \int_{t_0}^{\infty} dt \mathcal{H}_{i \nu \rightarrow i \nu'}^{T s} =: U_{i \nu \rightarrow i \nu'}^{(1) s}$ , this leads to the expressions given in the main text, where all  $2k_F$ -processes have been dropped. This is a good approximation (which has been checked numerically), because they always require at least one initial left-mover to tunnel. In the presence of interactions injected left-movers decay into a large left- and a small right-moving charge excitation (charge fractionalisation) and the spin excita-

tion moves completely to the left, because there are no interactions in the spin sector. In the particular geometry under consideration, where the injection point is on the left of the tunnel junction, this means that the tunneling of initial left-movers is strongly suppressed, because most of the excitation does not reach the junction. In the spin sector this is still valid for a beam splitter adiabatically coupled to Fermi liquid leads described by a  $g(x)$  model [59, 64, 65], whereas for the charge excitations additional reflections at the boundary to the Fermi liquid leads would appear. However, for generic length of the wires, we do not expect qualitative changes of the result.

## DIRECT CONTRIBUTIONS

The direct tunneling corrections of the current and of the current noise are

$$\begin{aligned}
I_1^{(2)\text{dir}} = & -e\Gamma_{2e} \sum_{\nu_1 \nu_2 \nu \nu' s} \frac{1 + \nu g}{2} \tag{S14} \\
& \times \left[ \|U_{2 \nu' \rightarrow 1 \nu}^{(1) s} | \nu_1 \uparrow, \nu_2 \downarrow \rangle\|^2 - \|U_{1 \nu \rightarrow 2 \nu'}^{(1) s} | \nu_1 \uparrow, \nu_2 \downarrow \rangle\|^2 \right],
\end{aligned}$$

$$S_{12}^{(2)\text{dir}} = -e^2 \Gamma_{2e} \sum_{\nu_1 \nu_2 \nu \nu' s} \frac{1 + \nu g}{2} \frac{1 + \nu' g}{2} \quad (\text{S15})$$

$$\times \text{Re} \left[ \|U_{2\nu' \rightarrow 1\nu}^{(1)s} |\nu_1 \uparrow, \nu_2 \downarrow\rangle\|^2 + \|U_{1\nu' \rightarrow 2\nu}^{(1)s} |\nu_1 \uparrow, \nu_2 \downarrow\rangle\|^2 \right].$$

We notice that the magnitude of these expressions is set by the standard quantum mechanical probability of the final state  $\|\cdot\|^2$ . This is in contrast to the exchange processes discussed in the main text, in which the magnitude is given by spin-flipped amplitudes, underlining the role of the exchange contribution as a nonclassical interference effect. Note that  $U$  only includes the part of the tunnel Hamiltonian denoted by its indices and is, therefore, not unitary.

The direct contributions are mostly constant, but they show additional features for certain injection points  $x_{1,2}$  (Fig. S1a,c).

The tunnel correction is always negative, because all tunnel events  $1 \rightarrow 2$  decrease the current after the junction, whereas  $2 \rightarrow 1$  increase it only if the electron becomes a right mover. The correction is weaker at higher interaction strength (smaller  $g$ ), which is related to the well-known suppression of the tunnel density of states in Tomonaga-Luttinger liquids (TLL) [55] and can be traced back to that fact that electrons are no eigenmodes of the theory.

In contrast to the exchange current, increasing the distance between the injection point and the tunnel junction does not suppress the direct current, because spin compensation is not required. As discussed in the main text, a charge (spin) imbalance across the junction gives rise to a charge (spin) average current. As a consequence there is a tunnel current even if the injected elec-

tron has completely disintegrated into spatially separated charge and spin modes by the time it reaches the junction. This holds even though the electron propagator  $\langle \Psi_\sigma(x, t) \Psi_\sigma^\dagger(0, 0) \rangle$  is algebraically suppressed in space  $x$  and time  $t$  (precisely due to spin-charge separation), because a Wick decomposition is not allowed in this interacting system.

Similar to the exchange current, there is a two-particle correlation effect: tunneling of charge excitations is suppressed if a charge or a spin excitation arrives simultaneously at the tunnel junction in the other wire. Two charge excitations can meet only if  $x_1 = x_2$ . In this case, both the in- and out-tunneling rates are reduced and so the total effect is very small. However, only charge out-tunneling is reduced if the charge excitation of electron 1 arrives simultaneously with the spin excitation of electron 2, i.e.,  $x_1/v_\rho = x_2/v_\sigma$ . Conversely, charge in-tunneling is reduced if the charge excitation of electron 2 meets the spin excitation of electron 1 at the junction, i.e.,  $x_1/v_\sigma = x_2/v_\rho$ . This produces secondary features, which are a signature of spin-charge separation (cf. Fig. S1a,c).

The current noise shows the same behavior, except that it is always reduced, irrespective of whether in- or out-tunneling is suppressed. This changes the sign of half the features, but leaves their position unchanged (Fig. S1c). The noise is negative, because due to charge conservation  $\delta I_1$  and  $\delta I_2$  have opposite signs in all processes.

Similar side dips have recently been found theoretically in the noise of collective excitations in chiral edge channels [46].

## ANALYTIC APPROXIMATION

The spin-flipped overlap integral  $P_{1 \rightarrow 2}$  used in the analytic approximation of the exchange current reads

$$P_{1 \rightarrow 2} := \sum_{t', t''} \langle \psi_{1R\uparrow}(x_1, t_0) \psi_{1R\uparrow}^\dagger(0, t'') \psi_{1R\downarrow}(0, t') \psi_{1R\downarrow}^\dagger(x_1, t_0) \rangle_1 \langle \psi_{2R\downarrow}(x_2, t_0) \psi_{2R\uparrow}(0, t'') \psi_{2R\downarrow}^\dagger(0, t') \psi_{2R\uparrow}^\dagger(x_2, t_0) \rangle_2$$

$$\propto \sum_{t', t''} \langle R \uparrow, R \downarrow | \text{T}_C \mathcal{H}_{1R \rightarrow 2R}^{T\downarrow}(t'^+) \mathcal{H}_{2R \rightarrow 1R}^{T\uparrow}(t''^-) | R \downarrow, R \uparrow \rangle. \quad (\text{S16})$$

Starting from Eq. (S12), this can be written as

$$P_{1 \rightarrow 2} \propto \sum_{t', t''} \left( \frac{i}{g} (t' - t'') + 1 \right)^{-\frac{g^{-1} + g}{2}} \left( i(t' - t'') + 1 \right)$$

$$\times \left( (x_1 + t')^2 + 1 \right)^{-\frac{1}{2}} \left( (x_1 + t'')^2 + 1 \right)^{-\frac{1}{2}} \left( (x_2 + t')^2 + 1 \right)^{-\frac{1}{2}} \left( (x_2 + t'')^2 + 1 \right)^{-\frac{1}{2}}$$

$$\times \exp \left[ i \frac{g^{-1} + g + 2}{4} \left( \arctan(x_1 + t'/g) - \arctan(x_1 + t''/g) - \arctan(x_2 + t'/g) + \arctan(x_2 + t''/g) \right) \right.$$

$$\left. + i \frac{g^{-1} + g - 2}{4} \left( \arctan(-x_1 + t'/g) - \arctan(-x_1 + t''/g) - \arctan(-x_2 + t'/g) + \arctan(-x_2 + t''/g) \right) \right], \quad (\text{S17})$$

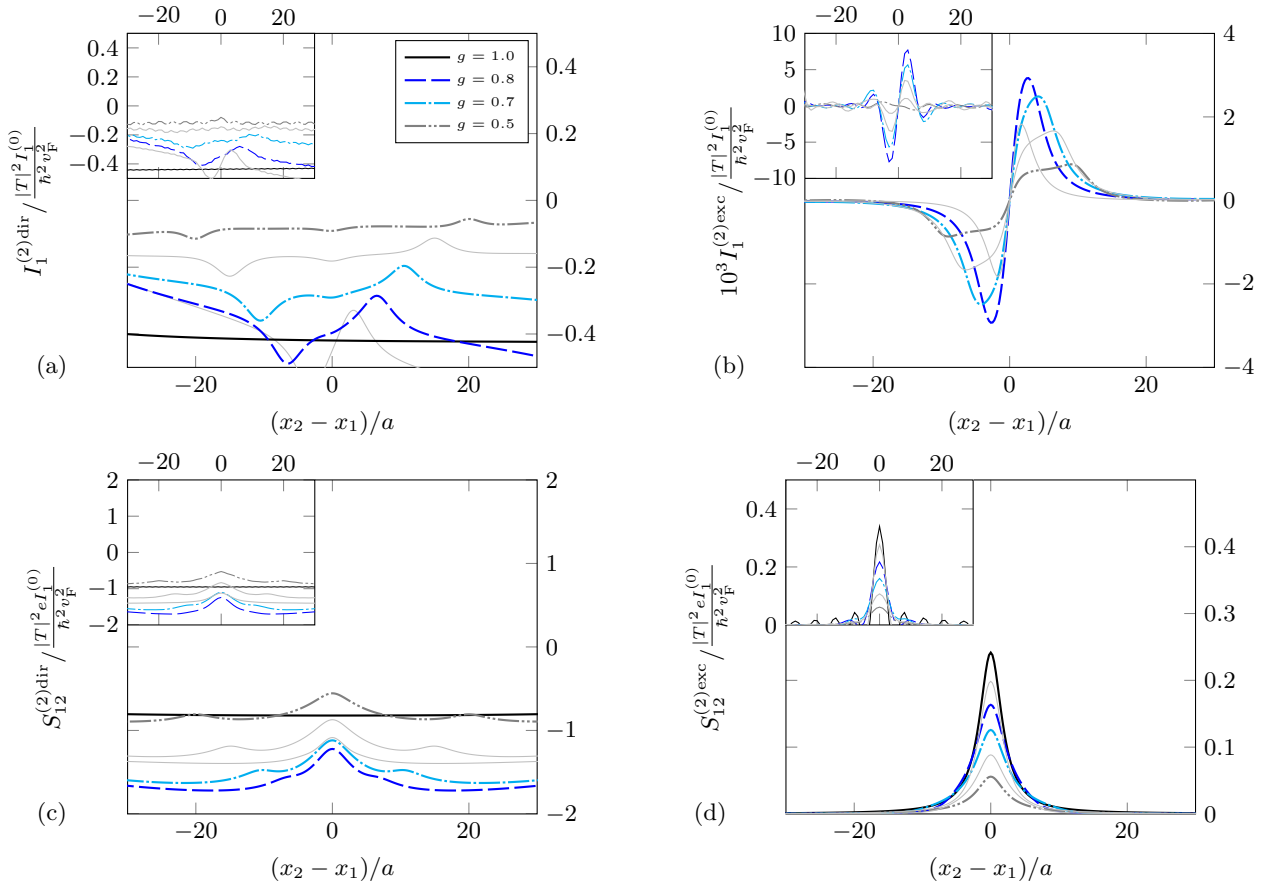


FIG. S1. (a) direct and (b) exchange current, (c) direct and (d) exchange current noise. Insets: a large voltage bias modeled as an injection Hamiltonian with a Peierls phase reproduces the initial state approximation for large voltages  $2eV \rightarrow \hbar v_F a^{-1}$  up to residual oscillations.

where we chose  $t_0 = 0$ . To extract the behavior at large injection distances, it suffices to consider absolute values and charge fractionalization can be dropped, because it is inessential for the spin exchange. So we discard the exponential factor, approximate  $g^{-1} + g + 2 \approx 4$  and perform a standard Taylor series expansion around  $(x_1 + x_2)^{-1} = 0$ .

### BIASED INJECTION

Instead of relying on the initial state approximation, the injection can be modeled by a second tunnel Hamiltonian which takes into account the voltage induced phase difference as a Peierls phase [70]:

$$\begin{aligned}
 H_I(t) &= I e^{i \frac{2eV}{\hbar} t} \sum_{\nu_1 \nu_2} \left[ \psi_{1\nu_1 \uparrow}(x_1, t) \psi_{2\nu_2 \downarrow}(x_2, t) \right. \\
 &\quad \left. + e^{i\varphi} \psi_{1\nu_1 \downarrow}(x_1, t) \psi_{2\nu_2 \uparrow}(x_2, t) \right] + \text{h.c.} \\
 &= I \sum_{\nu_1 \nu_2 \zeta} \left( \mathcal{H}_{\nu_1 \nu_2}^{I \text{dir}(\zeta)} + e^{i\varphi} \mathcal{H}_{\nu_1 \nu_2}^{I \text{exc}(\zeta)} \right). \quad (\text{S18})
 \end{aligned}$$

For sufficiently low injection rates there are no correlations between subsequently injected pairs and we can restrict the perturbative expansion to leading, i.e., second order in the injection amplitude  $I$ . Due to particle number conservation, tunneling and injection each enter at even orders only. All terms which are of zeroth order in the injection are equilibrium contributions and do not carry a current or cross-wire noise. The new generating functional is of the form

$$Z = Z^{(2I)} + Z^{(2I, 2T)} + \dots, \quad (\text{S19})$$

where the superscripts denote the expansion order in injection  $I$  and tunneling  $T$ . All expectation values are then taken with respect to the ground state. Special care has to be taken when contracting the Klein factors. Although not explicitly time dependent they need to be time-ordered which can introduce signs. The no-tunneling contributions are

$$I_1^{(2I)} = -\frac{ev_F}{a} \left| \frac{I}{\hbar v_F} \right|^2 \frac{\pi 2^{4\gamma}}{\Gamma(4\gamma)} \text{sgn}(V) \left| \frac{ea}{\hbar v_F} V \right|^{4\gamma-1}, \quad (\text{S20})$$

and

$$S_{12}^{(2I)} = \frac{e}{2} |I_1^{(2I)}|, \quad (\text{S21})$$

where  $\gamma = \frac{g^{-1}+g+2}{8}$ . The current shows a characteristic power law behavior which is expected since it applies to any TLL point injection calculation [58, 64]. Likewise,

the finite noise contribution is shot noise generated in the injection process. Note that the Schottky-like cross-correlation  $S_{12}$  does not contain an anomalous charge, which has been reported for the auto-correlation of infinite TLLs [58].

The leading order contributions are

$$I_1^{(2I,2T)\text{dir}} = -|I|^2|T|^2 \sum_{\lambda_i \nu_1 \nu_2 \nu_3 \nu'_s} \lambda_0 \lambda_1 \lambda_2 \lambda_3 \left( \frac{1+g}{2} (\lambda_0 - \lambda_1) + \frac{1+\nu g}{2} (\lambda_2 - \lambda_3) \right) \times \int \left( \prod_{m=1\dots 3} d\tau_m \right) \left\langle \text{Tr} \mathcal{H}_{\nu_1 \nu_2}^{\text{dir}}(0^{\lambda_0}) \mathcal{H}_{\nu_1 \nu_2}^{\text{dir}\dagger}(\tau_1^{\lambda_1}) \mathcal{H}_{1 \rightarrow 2, \nu \rightarrow \nu'}^{Ts}(\tau_2^{\lambda_2}) \mathcal{H}_{2 \rightarrow 1, \nu' \rightarrow \nu}^{Ts}(\tau_3^{\lambda_3}) \right\rangle, \quad (\text{S22})$$

$$I_1^{(2I,2T)\text{exc}} = -|I|^2|T|^2 \frac{1+g}{2} \sum_{\lambda_i} \lambda_0 \lambda_1 \lambda_2 \lambda_3 \left( (\lambda_0 - \lambda_1) + (\lambda_2 - \lambda_3) \right) \times \int \left( \prod_{m=1\dots 3} d\tau_m \right) \left\langle \text{Tr} \mathcal{H}_{RR}^{\text{dir}}(0^{\lambda_0}) \mathcal{H}_{RR}^{\text{exc}\dagger}(\tau_1^{\lambda_1}) \mathcal{H}_{1 \rightarrow 2, R \rightarrow R}^{T\downarrow}(\tau_2^{\lambda_2}) \mathcal{H}_{2 \rightarrow 1, R \rightarrow R}^{T\uparrow}(\tau_3^{\lambda_3}) \right\rangle, \quad (\text{S23})$$

$$S_{12}^{(2I,2T)\text{dir}} = \frac{|I|^2|T|^2}{2} \sum_{\substack{\lambda_i \nu_1 \nu_2 \\ \nu \nu'_s}} \lambda_0 \lambda_1 \lambda_2 \lambda_3 \left[ \left( (\lambda_0 - \lambda_1) \frac{1+g}{2} + (\lambda_2 - \lambda_3) \frac{1+\nu g}{2} \right) \left( (\lambda_0 - \lambda_1) \frac{1+g}{2} - (\lambda_2 - \lambda_3) \frac{1+\nu'g}{2} \right) \right] \times \int \left( \prod_{m=1\dots 3} d\tau_m \right) \left\langle \text{Tr} \mathcal{H}_{\nu_1 \nu_2}^{\text{dir}}(0^{\lambda_0}) \mathcal{H}_{\nu_1 \nu_2}^{\text{dir}\dagger}(\tau_1^{\lambda_1}) \mathcal{H}_{1 \rightarrow 2, \nu \rightarrow \nu'}^{Ts}(\tau_2^{\lambda_2}) \mathcal{H}_{2 \rightarrow 1, \nu' \rightarrow \nu}^{Ts}(\tau_3^{\lambda_3}) \right\rangle, \quad (\text{S24})$$

$$S_{12}^{(2I,2T)\text{exc}} = \frac{|I|^2|T|^2}{2} \left( \frac{1+g}{2} \right)^2 \sum_{\lambda_i} \lambda_0 \lambda_1 \lambda_2 \lambda_3 \left[ \left( (\lambda_0 - \lambda_1) + (\lambda_2 - \lambda_3) \right) \left( (\lambda_0 - \lambda_1) - (\lambda_2 - \lambda_3) \right) \right] \times \int \left( \prod_{m=1\dots 3} d\tau_m \right) \left\langle \text{Tr} \mathcal{H}_{RR}^{\text{dir}}(0^{\lambda_0}) \mathcal{H}_{RR}^{\text{exc}\dagger}(\tau_1^{\lambda_1}) \mathcal{H}_{1 \rightarrow 2, R \rightarrow R}^{T\downarrow}(\tau_2^{\lambda_2}) \mathcal{H}_{2 \rightarrow 1, R \rightarrow R}^{T\uparrow}(\tau_3^{\lambda_3}) \right\rangle, \quad (\text{S25})$$

where  $\lambda_i = \pm 1$  indicates which part of the Keldysh contour the time  $\tau^{\lambda_i}$  lies on. At large voltages, a numeric integration reproduces the results of the initial state approximation (Fig. S1, insets). The overlap integrals  $\mathcal{I} = \int d\tau \langle \dots \rangle$  are of the general form

$$\mathcal{I}(\{x\}, V, a) = \frac{1}{a^{\alpha+2}} \int \left( \prod_{m=1\dots 3} d\tau_m \right) e^{2iV\tau_1} \prod_n \left( i(x_n \pm v_n \tau_n) + a \right)^{\alpha_n}, \quad (\text{S26})$$

up to constant prefactors, where  $\alpha = \sum_n \alpha_n$ . With  $\eta$  a number we then derive the exact scaling law

$$\begin{aligned} \mathcal{I}(\{x\}, \eta V, a) &= \frac{1}{a^{\alpha+2}} \int \left( \prod_{m=1\dots 3} d\tau_m \right) e^{2i\eta V\tau_1} \prod_n \left( i(x_n \pm v_n \tau_n) + a \right)^{\alpha_n} \\ &= \frac{\eta^{-1}}{(\eta a)^{\alpha+2}} \int \left( \prod_{m=1\dots 3} d\tilde{\tau}_m \right) e^{2iV\tilde{\tau}_1} \prod_n \left( i(\eta x_n \pm v_n \tilde{\tau}_n) + \eta a \right)^{\alpha_n} \\ &= \eta^{-1} \mathcal{I}(\{\eta x\}, V, \eta a), \end{aligned} \quad (\text{S27})$$

where we have substituted  $\tilde{\tau} = \eta\tau$ . Assuming that the integral is independent of the high energy cutoff at low voltages and/or large injection distances, an approximate scaling law can be obtained by neglecting the scaling of  $a$  against that of  $i(x - v\tau)$ :

$$\begin{aligned} \mathcal{I}(\{x\}, \eta V, a) &= \frac{\eta^{-1}}{(\eta a)^{\alpha+2}} \int \left( \prod_{m=1\dots 3} d\tilde{\tau}_m \right) e^{2iV\tilde{\tau}_1} \prod_n \left( i(\eta x_n \pm v_n \tilde{\tau}_n) + \eta a \right)^{\alpha_n} \\ &\approx \frac{\eta^{-1}}{(\eta a)^{\alpha+2}} \int \left( \prod_{m=1\dots 3} d\tilde{\tau}_m \right) e^{2iV\tilde{\tau}_1} \prod_n \left( i(\eta x_n \pm v_n \tilde{\tau}_n) + a \right)^{\alpha_n} \\ &= \eta^{-3-\alpha} \mathcal{I}(\{\eta x\}, V, a). \end{aligned} \quad (\text{S28})$$

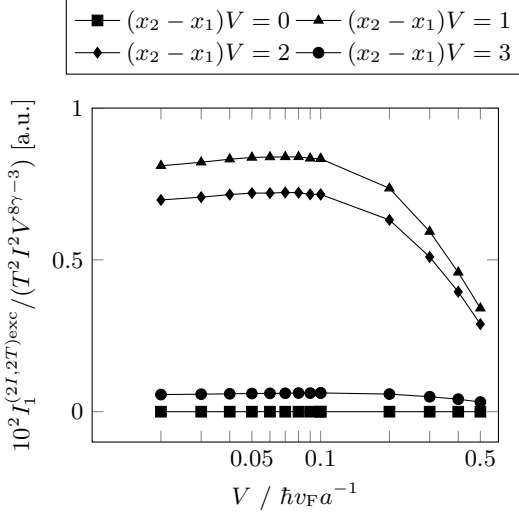


FIG. S2. When lowering the voltage and simultaneously rescaling  $x_1$  and  $x_2$ , the exchange current follows a power law. At large bias voltages,  $eV \gtrsim 0.1\hbar v_F a^{-1}$ , the influence of the high energy cutoff is still visible. The parameters are  $g = 0.8$  and  $(x_1 + x_2)V = -15a$ .

The validity of this approximation has been confirmed numerically (Fig. S2). Specifying  $\alpha$  leads to the scaling behavior given in the main text.

The scaling law implies that lowering the injection voltage corresponds to increasing all length scales, so the current-voltage relation  $I(V)$  (Fig. S3a) and the conductance-voltage relation  $G(V)$  (Fig. S3b) pick up the nonmonotonous behavior of the exchange current already present in Fig. 2. Therefore, it is not necessary in an experiment to actually change the injection points  $x_{1,2}$ .

## QUANTUM HALL DEVICE

Beam splitters have been successfully implemented as integer quantum Hall (QH) devices [42–45]. Cooper pair splitters are likely to suffer from the strong magnetic field, but recently a new correlated pair source for QH edge states has been realized [69], which may allow for

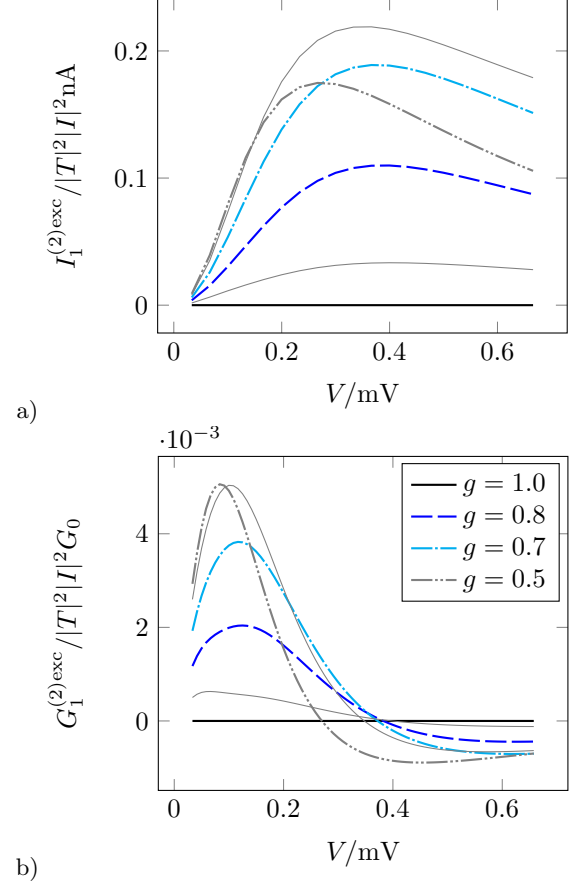


FIG. S3. a) Exchange current in wire 1 according to scaling relation (12) for different injection voltages and interaction parameters  $g$  within an experimentally realistic range. The injection points are fixed at  $x_1 = 1500$  nm,  $x_2 = 900$  nm. Gray lines represent equidistant intermediate  $g$  values. The material parameters are the same as in the main text. Note the nonmonotonous behavior similar to Fig. 2 in the main text. b) The corresponding conductance.

the injection of spin-entangled electrons. Concerning the beam splitter itself, a QH device offers considerable advantages. Being chiral, the edge state of the QH effect have a very large mean free path and a coherence length up to several  $10 \mu\text{m}$ . Chirality also implies the absence

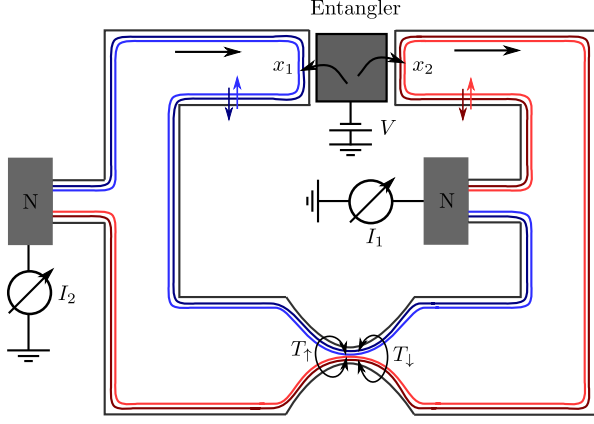


FIG. S4. Beam splitter realized in a quantum Hall sample of Corbino geometry. Two copropagating channels with opposite spin form a spinful chiral TLL at each edge. At a finite Zeeman splitting, they are spatially separated and the tunnel amplitudes at the constriction become spin dependent.

of charge fractionalization, which is an unwanted effect in our device. The intended geometry can be fabricated with high precision and fine tuned via appropriate gating in a running experiment thus giving immediate access to the injection distances  $|x_{1,2}|$ . Therefore we will explain how the results for the nanowires have to be modified in this section.

The beam splitter can be realized as a constriction in a ring-shaped Corbino QH sample (Fig. S4). The sample has to be operated at a Zeeman splitting much smaller than the Landau splitting, such that at each edge two copropagating channels of opposite spin form. Due to the difference in Zeeman energy, at a fixed Fermi energy opposite spins have different Fermi vectors and are slightly separated in real space. This has already been demonstrated experimentally [51]. When linearizing the spectrum around the Fermi points, where we assume the Fermi velocity  $v_F$  to be independent of edge and spin, the electrostatic repulsion between and within the channels can be treated exactly using bosonization. This yields two spinful chiral TLLs,

$$H_0 = \sum_{i\alpha} \int dx \hbar v_\alpha \left( \frac{\partial \phi_{i\alpha}}{\partial x} \right)^2, \quad (\text{S29})$$

where  $\alpha \in \{\rho, \sigma\}$  labels the charge and the spin channel at edge  $i \in \{1, 2\}$ . As in the nanowire, the charge velocity exceeds the spin velocity,  $v_\rho > v_\sigma = v_F$ . The electron field is  $\psi_{js}(x) = (2\pi a)^{-1/2} F_{js} \exp[ik_s x + 2\pi i \Phi_{js}(x)]$  where  $\Phi_{js} = \sqrt{\pi/2}(\phi_{j\rho} + s\phi_{j\sigma})$  with  $s \in \{\uparrow, \downarrow\}$  the spin

index and  $k_s$  the spin-dependent Fermi vector. The tunnel Hamiltonian becomes

$$\begin{aligned} H_T &= \sum_s \left( T_s \psi_{1s}^\dagger(0) \psi_{2s}(0) + T_s^* \psi_{2s}^\dagger(0) \psi_{1s}(0) \right) \\ &= \sum_s \left( T_s \mathcal{H}_{2 \rightarrow 1}^{T_s} + T_s^* \mathcal{H}_{1 \rightarrow 2}^{T_s} \right), \end{aligned} \quad (\text{S30})$$

where the tunnel amplitude  $T_s$  is in general complex because of the magnetic field and spin dependent, because at the constriction tunneling happens between the outer and the inner channels respectively (cf. Fig. S4). TLL behavior has already been investigated and observed in this system [46, 52].

The initial state is

$$\begin{aligned} |\varphi\rangle &= \sqrt{2\pi a} \left( \psi_{2\downarrow}^\dagger(x_2) \psi_{1\uparrow}^\dagger(x_1) + e^{i\varphi} \psi_{2\uparrow}^\dagger(x_2) \psi_{1\downarrow}^\dagger(x_1) \right) | \rangle \\ &:= 2^{-1/2} (|\uparrow, \downarrow\rangle + e^{i\varphi} |\downarrow, \uparrow\rangle). \end{aligned} \quad (\text{S31})$$

Lacking  $SU(2)$  spin invariance, the direct and exchange contributions have to be redefined as  $\frac{1}{2}(\langle \uparrow, \downarrow | \mathcal{O} | \uparrow, \downarrow \rangle + \langle \downarrow, \uparrow | \mathcal{O} | \downarrow, \uparrow \rangle)$  and  $\frac{1}{2}(e^{i\varphi} \langle \uparrow, \downarrow | \mathcal{O} | \downarrow, \uparrow \rangle + e^{-i\varphi} \langle \downarrow, \uparrow | \mathcal{O} | \uparrow, \downarrow \rangle)$ .

The calculation proceeds in analogy to the nanowire model and without further approximations one finds

$$\begin{aligned} I_1^{(2)\text{dir}} &= -e\Gamma_{2e} \frac{|T_\uparrow|^2 + |T_\downarrow|^2}{\hbar^2 v_F^2} \\ &\times \sum_s \left[ \|U_{2 \rightarrow 1}^{(1)s} | \uparrow, \downarrow \rangle\|^2 - \|U_{1 \rightarrow 2}^{(1)s} | \uparrow, \downarrow \rangle\|^2 \right], \end{aligned} \quad (\text{S32})$$

$$\begin{aligned} I_1^{(2)\text{exc}} &= e\Gamma_{2e} \frac{\text{Re}(T_\uparrow^* T_\downarrow e^{i(k_\uparrow - k_\downarrow)(x_1 - x_2) + i\varphi})}{\hbar^2 v_F^2} \\ &\times \left[ \langle \uparrow, \downarrow | U_{1 \rightarrow 2}^{(1)\uparrow\uparrow} U_{1 \rightarrow 2}^{(1)\downarrow\downarrow} | \downarrow, \uparrow \rangle - \langle \uparrow, \downarrow | U_{2 \rightarrow 1}^{(1)\downarrow\uparrow} U_{2 \rightarrow 1}^{(1)\uparrow\downarrow} | \downarrow, \uparrow \rangle \right], \end{aligned} \quad (\text{S33})$$

$$\begin{aligned} S_{12}^{(2)\text{dir}} &= -e^2 \Gamma_{2e} \frac{|T_\uparrow|^2 + |T_\downarrow|^2}{\hbar^2 v_F^2} \\ &\times \sum_s \left[ \|U_{2 \rightarrow 1}^{(1)s} | \uparrow, \downarrow \rangle\|^2 + \|U_{1 \rightarrow 2}^{(1)s} | \uparrow, \downarrow \rangle\|^2 \right], \end{aligned} \quad (\text{S34})$$

$$\begin{aligned} S_1^{(2)\text{exc}} &= -e\Gamma_{2e} \frac{\text{Re}(T_\uparrow^* T_\downarrow e^{i(k_\uparrow - k_\downarrow)(x_1 - x_2) + i\varphi})}{\hbar^2 v_F^2} \\ &\times \left[ \langle \uparrow, \downarrow | U_{1 \rightarrow 2}^{(1)\uparrow\uparrow} U_{1 \rightarrow 2}^{(1)\downarrow\downarrow} | \downarrow, \uparrow \rangle + \langle \uparrow, \downarrow | U_{2 \rightarrow 1}^{(1)\downarrow\uparrow} U_{2 \rightarrow 1}^{(1)\uparrow\downarrow} | \downarrow, \uparrow \rangle \right], \end{aligned} \quad (\text{S35})$$

where  $U_{j \rightarrow k}^{(1)s} = -i \int_{t_0}^\infty dt' \mathcal{H}^T(t')|_{j \rightarrow k}^s$  and the amplitudes are

$$\begin{aligned}
\langle \uparrow, \downarrow | \text{TC} \mathcal{H}_{1 \rightarrow 2}^{T_s}(t') \mathcal{H}_{2 \rightarrow 1}^{T_s}(t'') | \nu_1 \uparrow, \nu_2 \downarrow \rangle &= \frac{1}{4(2\pi)^2} \left[ f_\rho^{-1} f_\sigma^{-1} \right] (0, t'; 0, t'') \\
&\times \Xi_\uparrow(x_1, t_0^-; 0, t'') \Xi_\uparrow(x_1, t_0^+; 0, t') \Xi_\uparrow^{-1}(x_1, t_0^-; 0, t') \Xi_\uparrow^{-1}(x_1, t_0^+; 0, t'') \\
&\times \Xi_\downarrow(x_2, t_0^-; 0, t') \Xi_\downarrow(x_2, t_0^+; 0, t'') \Xi_\downarrow^{-1}(x_2, t_0^-; 0, t'') \Xi_\downarrow^{-1}(x_2, t_0^+; 0, t')
\end{aligned} \tag{S36}$$

and

$$\begin{aligned}
\langle \uparrow, \downarrow | \text{TC} \mathcal{H}_{1 \rightarrow 2}^{T_\downarrow}(t') \mathcal{H}_{2 \rightarrow 1}^{T_\uparrow}(t'') | \downarrow, \uparrow \rangle &= -\frac{a^2}{4(2\pi)^2} \left[ f_\rho^{-1} f_\sigma \right] (0, t'; 0, t'') \\
&\times \Xi_\uparrow(x_1, t_0^-; 0, t'') \Xi_\uparrow(x_1, t_0^+; 0, t') \Xi_\uparrow(x_2, t_0^-; 0, t'') \Xi_\uparrow(x_2, t_0^+; 0, t'') \\
&\times \Xi_\downarrow^{-1}(x_1, t_0^-; 0, t') \Xi_\downarrow^{-1}(x_1, t_0^+; 0, t'') \Xi_\downarrow^{-1}(x_2, t_0^-; 0, t'') \Xi_\downarrow^{-1}(x_2, t_0^+; 0, t').
\end{aligned} \tag{S37}$$

with

$$\Xi_s = f_\rho^{-\frac{1}{2}} f_\sigma^{-\frac{s}{2}} \tag{S38}$$

Up to quantitative corrections due to modified exponents we thus recover exactly the same behavior as in the nanowire case except that in the absence of backscattering, there are as many tunneling events which decrease the current after the junction as those which increase the current. So the direct contribution is zero up to the additional features which are induced by spin-charge separation as discussed in the nanowire case. Because the Fermi vectors for spin-up and spin-down are different, the exchange current acquires an oscillating prefactor. This is essentially the same mechanism as the one induced by the Rashba effect in nanowires, and likewise introduces an additional tunable parameter.

---

[1] M. A. Nielsen and I. L. Chuang, *Quantum Computation and Quantum Information* (Cambridge University Press, Cambridge, England, 2000).

[2] S. J. Freedman and J. F. Clauser, Phys. Rev. Lett. **28**, 938 (1972).

[3] A. Aspect, J. Dalibard, and G. Roger, Phys. Rev. Lett. **49**, 1804 (1982).

[4] G. Weihs, T. Jennewein, C. Simon, H. Weinfurter, and A. Zeilinger, Phys. Rev. Lett. **81**, 5039 (1998).

[5] J. S. Bell, Physics **1**, 195 (1964).

[6] J. F. Clauser, M. A. Horne, A. Shimony, and R. A. Holt, Phys. Rev. Lett. **23**, 880 (1969).

[7] D. Loss and D. P. DiVincenzo, Phys. Rev. A **57**, 120 (1998).

[8] R. Hanson, L. P. Kouwenhoven, J. R. Petta, S. Tarucha, and L. M. K. Vandersypen, Rev. Mod. Phys. **79**, 1217 (2007).

[9] P. Recher, E. V. Sukhorukov, and D. Loss, Phys. Rev. B **63**, 165314 (2001).

[10] G. Lesovik, T. Martin, and G. Blatter, Eur. Phys. J. B **24**, 287 (2001).

[11] P. Recher and D. Loss, Phys. Rev. B **65**, 165327 (2002).

---

[12] C. Bena, S. Vishveshwara, L. Balents, and M. P. A. Fisher, Phys. Rev. Lett. **89**, 037901 (2002).

[13] P. Recher and D. Loss, Phys. Rev. Lett. **91**, 267003 (2003).

[14] A. Levy Yeyati, F. S. Bergeret, A. Martin-Rodero, and T. M. Klapwijk, Nat. Phys. **3**, 455 (2007).

[15] J. Cayssol, Phys. Rev. Lett. **100**, 147001 (2008).

[16] K. Sato, D. Loss, and Y. Tserkovnyak, Phys. Rev. Lett. **105**, 226401 (2010).

[17] J. Torrès and T. Martin, Eur. Phys. J. B **12**, 319 (1999).

[18] G. Falci, D. Feinberg, and F. W. J. Hekking, Europhys. Lett. **54**, 255 (2001).

[19] L. Hofstetter, S. Csonka, J. Nygård, and C. Schönenberger, Nature (London) **461**, 960 (2009).

[20] L. G. Herrmann, F. Portier, P. Roche, A. Levy Yeyati, T. Kontos, and C. Strunk, Phys. Rev. Lett. **104**, 026801 (2010).

[21] A. Das, Y. Ronen, M. Heiblum, D. Mahalu, A. V. Kretinin, and H. Shtrikman, Nat. Commun. **3**, 1165 (2012).

[22] J. Schindele, A. Baumgartner, and C. Schönenberger, Phys. Rev. Lett. **109**, 157002 (2012).

[23] S. Kawabata, J. Phys. Soc. Jpn. **70**, 1210 (2001).

[24] N. M. Chtchelkatchev, G. Blatter, G. B. Lesovik, and T. Martin, Phys. Rev. B **66**, 161320 (2002).

[25] P. Samuelsson, E. V. Sukhorukov, and M. Büttiker, Phys. Rev. Lett. **91**, 157002 (2003).

[26] C. W. J. Beenakker, C. Emary, M. Kindermann, and J. L. van Velsen, Phys. Rev. Lett. **91**, 147901 (2003).

[27] P. Samuelsson, E. V. Sukhorukov, and M. Büttiker, Phys. Rev. Lett. **92**, 026805 (2004).

[28] O. Sauret, T. Martin, and D. Feinberg, Phys. Rev. B **72**, 024544 (2005).

[29] W. Chen, R. Shen, L. Sheng, B. G. Wang, and D. Y. Xing, Phys. Rev. Lett. **109**, 036802 (2012).

[30] B. Braunecker, P. Burset, and A. Levy Yeyati, Phys. Rev. Lett. **111**, 136806 (2013).

[31] G. Burkard, D. Loss, and E. V. Sukhorukov, Phys. Rev. B **61**, R16303 (2000).

[32] J. C. Egues, G. Burkard, and D. Loss, Phys. Rev. Lett. **89**, 176401 (2002).

[33] G. Burkard and D. Loss, Phys. Rev. Lett. **91**, 087903 (2003).

- (2003).
- [34] X. Hu and S. Das Sarma, Phys. Rev. B **69**, 115312 (2004).
- [35] P. Samuelsson, E. V. Sukhorukov, and M. Büttiker, Phys. Rev. B **70**, 115330 (2004).
- [36] J. C. Egues, G. Burkard, D. S. Saraga, J. Schliemann, and D. Loss, Phys. Rev. B **72**, 235326 (2005).
- [37] V. Giovannetti, D. Frustaglia, F. Taddei, and R. Fazio, Phys. Rev. B **74**, 115315 (2006).
- [38] P. San-Jose and E. Prada, Phys. Rev. B **74**, 045305 (2006).
- [39] F. Mazza, B. Braunecker, P. Recher, and A. Levy Yeyati, Phys. Rev. B **88**, 195403 (2013).
- [40] A. Komnik and R. Egger, Phys. Rev. Lett. **80**, 2881 (1998).
- [41] A. Komnik and R. Egger, Eur. Phys. J. B **19**, 271 (2001).
- [42] Y. Ji, Y. Chung, D. Sprinzak, M. Heiblum, D. Mahalu, and H. Shtrikman, Nature (London) **422**, 415 (2003).
- [43] I. Neder, M. Heiblum, Y. Levinson, D. Mahalu, and V. Umansky, Phys. Rev. Lett. **96**, 016804 (2006).
- [44] I. Neder, N. Ofek, Y. Chung, M. Heiblum, D. Mahalu, and V. Umansky, Nature (London) **448**, 333 (2007).
- [45] E. Bocquillon, V. Freulon, J.-M. Berroir, P. Degiovanni, B. Plaçais, A. Cavanna, Y. Jin, and G. Fève, Science **339**, 1054 (2013).
- [46] C. Wahl, J. Rech, T. Jonckheere, and T. Martin, Phys. Rev. Lett. **112**, 046802 (2014).
- [47] S.-i. Tomonaga, Prog. Theor. Phys. **5**, 544 (1950).
- [48] J. M. Luttinger, J. Math. Phys. **4**, 1154 (1963).
- [49] J. Kim, K. Kang, J.-O. Lee, K.-H. Yoo, J.-R. Kim, J. W. Park, H. M. So, and J.-J. Kim, J. Phys. Soc. Jpn. **70**, 1464 (2001).
- [50] B. Gao, A. Komnik, R. Egger, D. C. Glattli, and A. Bachtold, Phys. Rev. Lett. **92**, 216804 (2004).
- [51] B. Karmakar, D. Venturelli, L. Chirolli, F. Taddei, V. Giovannetti, R. Fazio, S. Roddaro, G. Biasiol, L. Sorba, V. Pellegrini, and F. Beltram, Phys. Rev. Lett. **107**, 236804 (2011).
- [52] E. Bocquillon, V. Freulon, J.-M. Berroir, P. Degiovanni, B. Plaçais, A. Cavanna, Y. Jin, and G. Fève, Nat. Commun. **4**, 1839 (2013).
- [53] J. von Delft and H. Schoeller, Ann. Phys. (Berlin) **7**, 225 (1998).
- [54] H. Grabert, in *Exotic States in Quantum Nanostructures*, edited by S. Sarkar (Kluwer Academic Publishers, Dordrecht, 2002) Chap. 1.
- [55] T. Giamarchi, *Quantum Physics in One Dimension* (Oxford University Press, 2003).
- [56] In a spinless TLL at sufficiently strong interactions,  $g < 1/2$ , electrostatic interwire effects become relevant (in the renormalization group sense), which change the model substantially [40]. Additional noninteracting channels like spin lower this bound [50], but we shall conservatively limit this discussion to moderate interaction strengths  $1/2 < g \leq 1$ .
- [57] C. L. Kane and M. P. A. Fisher, Phys. Rev. Lett. **72**, 724 (1994).
- [58] A. Crépieux, R. Guyon, P. Devillard, and T. Martin, Phys. Rev. B **67**, 205408 (2003).
- [59] F. Dolcini, B. Trauzettel, I. Safi, and H. Grabert, Phys. Rev. B **71**, 165309 (2005).
- [60] K.-V. Pham, M. Gabay, and P. Lederer, Phys. Rev. B **61**, 16397 (2000).
- [61] D. L. Maslov and M. Stone, Phys. Rev. B **52**, R5539 (1995).
- [62] V. V. Ponomarenko, Phys. Rev. B **52**, R8666 (1995).
- [63] I. Safi and H. J. Schulz, Phys. Rev. B **52**, R17040 (1995).
- [64] A. V. Lebedev, A. Crépieux, and T. Martin, Phys. Rev. B **71**, 075416 (2005).
- [65] P. Recher, N. Y. Kim, and Y. Yamamoto, Phys. Rev. B **74**, 235438 (2006).
- [66] S. Ol'khovskaya, J. Splettstoesser, M. Moskalets, and M. Büttiker, Phys. Rev. Lett. **101**, 166802 (2008).
- [67] Spin excitations do, however, create charge noise.
- [68] If a spin-up electron tunnels, there cannot be any overlap with the spin-flipped state, as the total spin per wire does not vanish. The event is explicitly ruled out by Klein factors in Eq. (6).
- [69] N. Ubbelohde, F. Hohls, V. Kashcheyevs, T. Wagner, L. Fricke, B. Kästner, K. Pierz, H. W. Schumacher, and R. J. Haug, Nat. Nanotechnol., advance online publication (2014), arXiv:1404.0030.
- [70] G. D. Mahan, *Many-Particle Physics* (Kluwer Academic/Plenum Publishers, New York, 1981).
- [71] Y. A. Bychkov and E. I. Rashba, J. Phys. C **17**, 6039 (1984).
- [72] D. Liang and X. P. Gao, Nano Lett. **12**, 3263 (2012).
- [73] Y. Kanai, R. S. Deacon, S. Takahashi, A. Oiwa, K. Yoshida, K. Shibata, K. Hirakawa, Y. Tokura, and S. Tarucha, Nat. Nanotech. **6**, 511 (2011).
- [74] P. Wójcik, J. Adamowski, B. J. Spisak, and M. Wołoszyn, J. Appl. Phys. **115**, 104310 (2014).